CONFERENCE PRE-PRINT

RECOVERY BEHAVIOR OF HIGH-PURITY CUBIC SIC FOR FIRST-WALL APPLICATIONS IN FUSION REACTORS BY POST-IRRADIATION ANNEALING AFTER LOW-TEMPERATURE NEUTRON IRRADIATION

Mohd Idzat Idris
Nuclear Technology Research Center, Faculty of Science and Technology, Universiti Kebangsaan Malaysia, 43600 Bangi Selangor, Malaysia
Email: idzat@ukm.edu.my

Katsumi Yoshida & Toyohiko Yano
Institute of Integrated Resarch, Laboratory for Zero-Carbon Energy, Institute of Science 2-12-1, Ookayama, Meguro-ku, Tokyo, 152-8550 Japan

Abstract

This study examines the defect recovery behavior of two types of high-purity cubic silicon carbide (β-SiC) polycrystals, namely PureBeta-SiC and CVD-SiC, following low-temperature neutron irradiation in the BR2 reactor (Belgium). Samples were exposed to a fluence of 2.1×10^{24} n/m² (E > 0.1 MeV) at 340 K, then subjected to stepwise thermal annealing up to 1673 K in a helium atmosphere. In-situ dilatometry was used to measure macroscopic length recovery, and activation energies for defect recombination were extracted using first-order kinetic models. Four distinct recovery stages were identified with corresponding activation energies: 0.19–0.23 eV (373–573 K), 0.01–0.04 eV (673–873 K), 0.24–0.30 eV (923–1223 K), and 1.30–1.35 eV (1323–1523 K). More than 70% of volume recovery occurred below 1223 K, attributed to the recombination of closely spaced Frenkel pairs. Higher temperatures facilitated longer-range migration, particularly of silicon interstitials. Comparative results indicate that β-SiC demonstrates enhanced recovery efficiency relative to hexagonal α-SiC below 873 K.

1. INTRODUCTION

Silicon carbide (SiC) is widely recognised for its superior thermal and mechanical properties, including high-temperature stability above 1273 K and strength exceeding 600 MPa [1,2]. These qualities make it an attractive candidate for use in nuclear environments, particularly in TRISO fuel particles for high-temperature gas-cooled reactors [3,4]. SiC also finds applications in high-stress industrial environments, such as combustion engines [5], magnetohydrodynamic generators [6], power semiconductors [7], and transport systems [8]. However, the brittle nature of monolithic SiC remains a major drawback, limiting its structural reliability under mechanical loading.

To improve damage tolerance, silicon carbide fibre-reinforced composites (SiCf/SiC) have been developed, integrating a SiC matrix into woven SiC fibre preforms. These composites demonstrate enhanced toughness and irradiation resistance and are under consideration for cladding, structural internals, and blanket materials in both fission and fusion reactors [9,10]. Fusion environments, especially near the first wall, expose materials to intense neutron flux, heat, and high-energy ions, which can cause severe displacement damage and material degradation [11]. Studying the post-irradiation recovery behaviour of SiC is therefore essential to understanding the thermal and defect stability of these materials under reactor conditions.

In this study, we examine the recovery kinetics of two high-purity monolithic β-SiC polycrystals—PureBeta and CVD-SiC—following neutron irradiation in the BR2 reactor at ~340 K to a fluence of 2.1×10^{24} n/m². Building on previous work that characterised dimensional and structural changes in irradiated SiC variants [12], we employed stepwise thermal annealing up to 1673 K and in-situ dilatometry to track macroscopic recovery. By analysing recovery behaviour across temperature intervals, we aim to identify the underlying defect recombination mechanisms and evaluate the thermal resilience of β-SiC for nuclear structural.

2.0 EXPERIMENTAL PROCEDURES

2.1 Materials

This study utilised two types of high-purity β-phase silicon carbide (β-SiC) polycrystals: PureBeta-SiC and chemical vapour deposited (CVD)-SiC, to evaluate defect recovery following neutron irradiation. PureBeta-SiC, supplied by Bridgestone Corporation (Japan), is produced through advanced polymer-derived ceramic processing and sintered using a non-metallic binder via hot pressing above 2273 K. The final product exhibits a high theoretical density (~98%, 3.14 g/cm³), with trace carbon inclusions at grain boundaries and total metallic impurities below 0.3 ppm [13]. CVD-SiC, obtained from Rohm and Haas Advanced Materials (USA), is synthesised through gas-phase deposition in the temperature range of 1173–1373 K, yielding a fully dense, single-phase cubic β-SiC with a purity exceeding 99.9995% and negligible porosity or microcracking [14,15]. All specimens were fabricated into rectangular bars of dimensions 25 mm × 4 mm × 2 mm for subsequent irradiation and analysis.

2.2 Neutron Irradiation and Thermal Annealing

Both SiC variants were simultaneously irradiated in the BR2 reactor (SCK CEN, Belgium) under identical conditions. The irradiation was performed at a nominal temperature of 340 ± 10 K for a duration of 60 days, achieving a fast neutron fluence of approximately 2.1×10^{24} n/m² (E > 0.1 MeV), equivalent to 0.21–0.25 displacements per atom (dpa). Post-irradiation, each bar was sectioned into smaller coupons (25 mm × 2 mm × 2 mm) for annealing measurements. The annealing study was conducted using a high-resolution dilatometer (DIL 402C, NETZSCH, Germany) in a flowing helium environment. Isochronal annealing was performed from room temperature up to 1673 K in 50 K increments, with each temperature step maintained for 6 hours. The instrument recorded in-situ changes in specimen length with a resolution of 10 nm, corresponding to a relative precision of 0.00004% for a 25 mm sample. After completing the thermal cycle, macroscopic length recovery was confirmed by micrometry, and crystallographic recovery was assessed via room-temperature X-ray diffraction (XRD), as described in previous work [12].

2.3 Analysis of Recovery Kinetics

Thermal annealing facilitates the recovery of neutron-induced defects by promoting the recombination of Frenkel pairs—interstitial-vacancy combinations formed during irradiation. The extent of volume recovery (ΔV) reflects the elimination of such defects and can be modelled using a first-order kinetic expression. By assuming defect recombination as a thermally activated process, the rate constant k can be extracted from isothermal annealing data and fitted to an Arrhenius-type relationship to determine the activation energy (E_a):

$$\ln[A] - \ln[A_0] = -kt$$

$$\ln k = -\frac{E_a}{k_B T} + \ln A$$

where A_0 and A represent the initial and time-dependent defect-related volume, k_B is the Boltzmann constant, and T is the absolute temperature. This approach enables quantification of the energy barriers associated with defect migration and recombination in irradiated β-SiC.

3. RESULTS AND DISCUSSION

3.1 Isochronal Annealing Behaviour

Figure 1 presents the dimensional recovery of PureBeta-SiC and CVD-SiC during 6-hour isochronal annealing from room temperature to 1673 K. Both materials exhibited comparable recovery patterns, initiating at approximately 340 K—close to the irradiation temperature—and continuing with a marked increase up to ~573 K. This suggests that the majority of irradiation-induced defects were mobile at relatively low temperatures. Beyond 573 K, the rate of length recovery diminished, with recovery approaching saturation near 1573 K. This behaviour implies that the predominant irradiation damage consisted of isolated point defects and small defect clusters, consistent with the low-temperature, moderate-fluence irradiation condition.

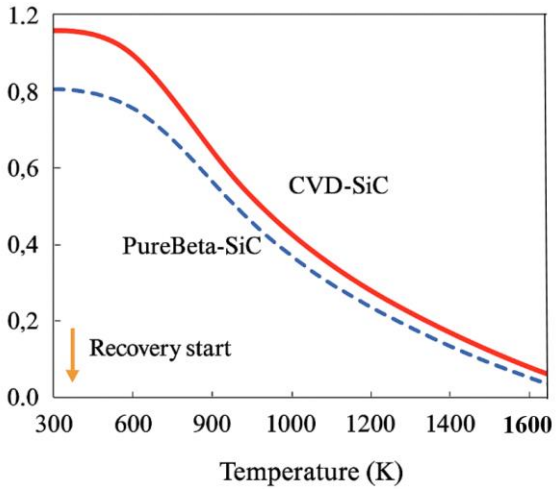

Figure 1. Recovery behavior by isochronal annealing from room temperature up to 1673 K

The observed recovery onset near the irradiation temperature agrees with earlier studies, which found that swelling induced in SiC by neutron exposure begins to reverse once the annealing temperature surpasses the irradiation condition [17,18]. Similar behaviour was noted in β- and α-SiC samples exposed to varying fluences at temperatures below 773 K [16]. To further assess structural recovery, X-ray diffraction (XRD) was used to monitor shifts in lattice spacing at room temperature. Figure 2 displays the XRD peaks for several key crystallographic planes, with post-annealed samples showing restored peak positions corresponding to their unirradiated counterparts—indicating near-complete lattice recovery.

Quantitative analysis of both macroscopic length and lattice parameter confirms that full recovery was nearly achieved at 1673 K, although over 90% recovery had already occurred by 1573 K. When compared with recovery in hexagonal (6H) α-SiC containing boron additives [24], β-SiC exhibited a significantly faster recovery at temperatures below ~873 K, especially under 573 K, reinforcing the hypothesis that β-SiC is more susceptible to low-temperature defect recombination.

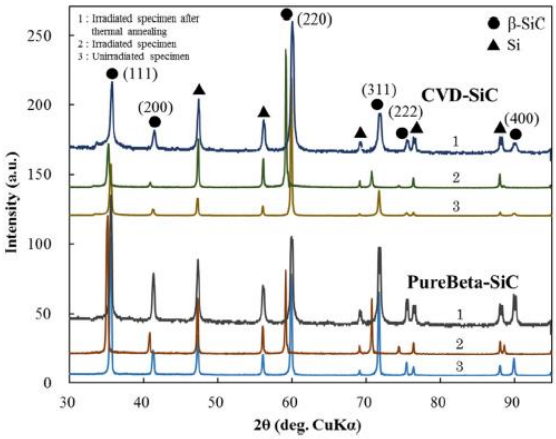

Figure 2.XRD profile peaks measured at room temperature after post-irradiation annealing

3.2 Isothermal Annealing and Activation Energy

To probe the kinetics of defect recovery, isothermal annealing experiments were conducted at selected temperatures for 6-hour durations. Figure 3 shows logarithmic plots of volumetric recovery for PureBeta-SiC at 473 K and CVD-SiC at 1073 K. The data were divided into two linear regions (early and late stages) to better fit first-order kinetic models. Rate constants (k) were extracted from these slopes, with determination coefficients (R^2) typically exceeding 0.95. A brief thermal overshoot was observed at the beginning of each temperature step

(~15 minutes), particularly at lower temperatures, and these segments were excluded from kinetic fitting, as recommended by Yamazaki et al. [16].

Arrhenius plots of the calculated rate constants across temperatures reveal distinct stages of defect recovery, indicating the involvement of different defect species and recombination mechanisms. For PureBeta-SiC, four stages were identified: Stage I (373–573 K), Stage II (673–873 K), Stage III (923–1223 K), and Stage IV (1323–1523 K). The corresponding activation energies ranged from ~0.19 eV in Stage I to ~1.38 eV in Stage IV. CVD-SiC followed a similar trend, though the data were analysed up to 1573 K due to signal fluctuations at higher temperatures. The near-flat slope in Stage II suggests a temperature-insensitive recombination mechanism, possibly involving pre-existing, closely associated Frenkel pairs.

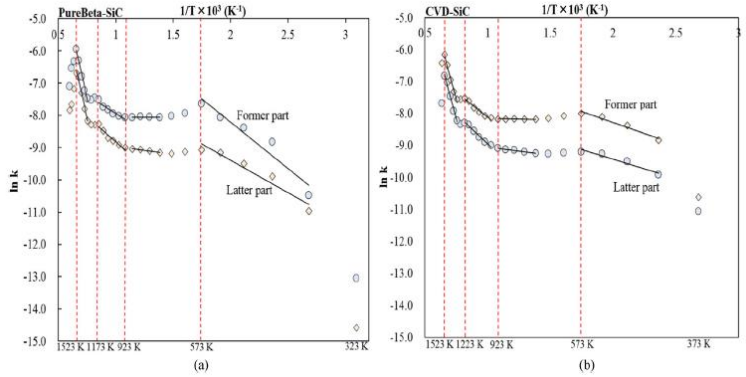

Figure 3. The Arrhenius plot of volume recovery of PureBeta-SiC and CVD-SiC according to the rate coefficient, k value which obtained by first order reaction

Activation energy values for each stage (Table 1) closely align with those reported in prior studies for high-purity SiC [20], and deviations in activation energies reported for SiC doped with B_4C or Al_2O_3 were attributed to impurity interactions [21–23]. The β-SiC samples in this study demonstrated faster low-temperature recovery (Stages I and II) compared to α-SiC, indicating a potential advantage for β-SiC in applications requiring dimensional stability under low thermal budgets.

Table 1. Activation energies of PureBeta-SiC and CVD-SiC by first order reaction

Activation energies (eV)			
Specimen	Temperature range (K)	1st Order reaction	
		Former part	Latter part
PureBeta	373–573	0.24	0.17
	723–923	0.002	0.04
	923–1173	0.20	0.27
	1323–1523	1.38	1.37
CVD-SiC	423–573	0.12	0.10
	723–923	0.006	0.04
	973–1223	0.26	0.31
	1323–1473	1.26	1.29

Simulation studies by Weber and Gao [25,26] using molecular dynamics support the observed recombination energetics. Carbon Frenkel pairs exhibit recombination energies between 0.24 and 1.6 eV, while silicon pairs require 0.28 to 0.90 eV. Interstitial migration energies were found to be ~0.74 eV for carbon and ~1.53 eV for silicon [27], whereas vacancy migration required significantly higher energy—4.10 eV for carbon and 2.35 eV for silicon—values not observed in this study, indicating that migration of isolated vacancies is negligible below 1523 K.

The highest activation energy observed (~1.38 eV for PureBeta-SiC) matches values associated with long-range Si interstitial migration or recombination of more widely spaced C Frenkel pairs [28,29]. This suggests that at higher annealing temperatures (Stage IV), recovery involves extended-range defect interactions, whereas earlier stages are governed by recombination of closely positioned defects. Supporting this, nearly three-fourths of the

total volume recovery occurred by 1223 K, indicating minimal need for long-range migration in most of the recovery process.

Notably, no evidence of vacancy migration was detected, consistent with prior findings that void formation in SiC typically occurs at temperatures above 1523 K [30]. However, subtle signs of void nucleation near stacking faults have been observed at slightly lower temperatures (~1403 K) via TEM imaging [31], suggesting that localised sinks might facilitate recovery in some regions. The relatively flat recovery rate in intermediate temperature intervals (573–923 K and 1173–1323 K) remains an open question but is consistent with other reports of non-monotonic recovery behaviour in SiC [20,24].

4. CONCLUSION

In this study, high-purity cubic silicon carbide polycrystals, namely PureBeta-SiC and CVD-SiC, were simultaneously irradiated in the BR2 reactor (Belgium) to a neutron fluence of approximately $2.0–2.5 \times 10^{24}$ n/m² ($E > 0.1$ MeV) at temperatures ranging from 333 to 363 K. The recovery of irradiation-induced defects was systematically investigated through isochronal and isothermal annealing up to 1673 K. The key findings are summarised below:

1. **Multi-stage recovery kinetics:** Both β-SiC materials exhibited four distinct recovery stages, each characterised by different activation energies. For PureBeta-SiC and CVD-SiC, the activation energies were estimated as follows:
   – Stage I (373–573 K): 0.17–0.24 eV and 0.12–0.14 eV
   – Stage II (723–923 K): 0.002–0.04 eV and 0.006–0.04 eV
   – Stage III (923–1223 K): 0.20–0.27 eV and 0.26–0.31 eV
   – Stage IV (1323–1523 K): 1.37–1.38 eV and 1.26–1.29 eV
2. **Defect recombination mechanisms:** A majority of recovery—approximately 75%—occurred below 1223 K, likely due to recombination of closely spaced carbon and silicon Frenkel pairs, without requiring significant long-range migration. At elevated temperatures (1323–1523 K), recovery appears to involve more spatially separated C interstitials and thermally activated migration of Si interstitials. No evidence of independent carbon or silicon vacancy migration was observed within the annealing range, suggesting that vacancies act primarily as recombination sinks up to 1523 K.
3. **Comparison with hexagonal SiC:** When compared to hexagonal α-SiC, high-purity β-SiC demonstrated a more pronounced recovery in the low-temperature region. In particular, β-SiC showed accelerated dimensional restoration below 873 K, with a significant portion occurring under 573 K, indicating its superior defect mobility at lower thermal budgets.

These results reinforce the potential of high-purity β-SiC for advanced nuclear applications, especially in systems where efficient recovery at moderate temperatures is critical for structural integrity and longevity.

ACKNOWLEDGEMENTS

This work was partially funded by the Grant-in-Aid for Scientific Research from the Japan Society for the Promotion of Science (JSPS), and was additionally supported by the Japan Atomic Energy Agency (JAEA) under the framework of the ITER Broader Approach (BA) activities. The authors gratefully acknowledge the assistance provided by the staff of the International Research Center for Nuclear Materials Science, Institute for Materials Research, Tohoku University, in conducting the neutron irradiation experiments.

REFERENCES

[1] Product sheet from Rohm and Haas Co. http://www.dow.com/assets/attachments/business/gt/advanced_ceramics/cvd_silicon_carbide/tds/cvd_silicon_carbide.pdf, 9 October 2014.

[2] Ultra high purity fine ceramics (SiC) component PureBeta**,** http://www.bridgestone.com/products/diversified/purebeta/sic/specifications.html, 9 October 2014.

[3] S. Ueta, J. Aihara, N. Sakaba, M. Honda, N. Furihara, K. Sawa, J. Nucl. Sci. Technol. 51 (2014) 1345-1354.

[4] J. Aihara, S. Ueta, M. Honda, P. Blynskiy, S. Gizatulin, N. Sakaba, Y. Tachibana, J. Nucl. Sci. Technol. 51 (2014) 1355-1363.

[5] S. Wodin-Schwartz, D.R. Myers, R.K. Kramer, S. Choi, A. Jordan, M.B.J. Wijesundara, M.A. Hopcroft, A.P. Pisano, Proc. Power MEMS. (2008) 477-480.

[6] T. Okuo, T. Ookouchi, Y. Aoki, A SiC-CuG-Cu insulator for MHD generator channels, IEEE Service Center, New Jersey, 1989, pp. 67-68.

[7] K. Shenai, Proc. of the IEEE. (2000) 516-523.

[8] Y. Katoh, H. Kishimoto, A. Kohyama, Mater. Trans. 43 (2002) 612-616.

[9] A. Ivekovic, S. Novak, G. Drazic, D. Blagoeva, S.G.D. Vicente, J. Eur. Ceram. Soc. 33 (2013) 1577-1589.

[10] Y. Katoh, K. Ozawa, C. Shih, T. Nozawa, R.J. Shinavski, A. Hasegawa, L.L. Snead, J. Nucl. Mater. 448 (2014) 448–476.

[11] L.L. Snead, T. Nozawa, M. Ferraris, Y. Katoh, R. Shinavski, M. Sawan, J. Nucl. Mater. 417 (2011) 330-339.

[12] M.I. Idris, H. Konishi, M. Imai, K. Yoshida and T. Yano, Energy Procedia, [In print].

[13] http://www.bridgestone.com/products/diversified/purebeta/quality_service.html#process, 9 October 2014.

[14] L.L. Snead, T. Nozawa, Y. Katoh, T. Byun, S. Kondo, D.A. Petti, J. Nucl. Mater. 371 (2007) 329-377. http://www.dow.com/assets/attachments/business/gt/advanced_ceramics/cvd_silicon_carbide/tds/cvd_silicon_carbide.pdf, 9 October 2014.

[15] S. Yamazaki, M. Imai, T. Yano, Prog. Nucl. Energy. 50 (2008) 601-605.

[16] N.F. Pravdyuk, V.A. Nikolaenko, V.I. Kapuchin, V.N. Kusnetsov, Properties of reactor materials and the effects of radiation damage, in: D. J. Littler (Eds.), Proceedings of the International Conference at Berkeley Castle, Butterworths, London, 1962, pp. 57.

[17] T. Yano, M. Akiyoshi, K. Ichikawa, Y. Tachi, T. Iseki, J. Nucl. Mater. 289 (2001) 102-109.

[18] T. Sawabe, M. Akiyoshi, K. Yoshida, T. Yano, J. Nucl. Mater. 417 (2011) 430-434.

[19] T. Yano, Y. You, K. Kanazawa, T. Kobayashi, M. Imai, K. Yoshida, S. Yamazaki, J. Nucl. Mater. 455 (2014) 445-449.

[20] T. Suzuki, T. Yano, T. Maruyama, T. Iseki. T. Mori, J. Nucl. Mater. 165 (1989) 247-251.

[21] T. Suzuki, T. Iseki. T. Mori, J.H. Evans, J. Nucl. Mater. 170 (1990) 113-116.

[22] S. Yamazaki, K. Yoshida, T. Yano, J. Nucl. Mater. 417 (2011) 425-429.

[23] T. Yano, Y. Futamura, S. Yamazaki, T. Sawabe, K. Yoshida, J. Nucl. Mater. 442 (2013) S399-S403.

[24] W.J. Weber, F. Gao, R. Devanathan, W. Jiang, C.M. Wang, Nucl. Instrum. Methods Phys. Res. B 216 (2004) 25-35.

[25] F. Gao, W.J. Weber, J. Appl. Phys. 94 (2003) 4348-4356.

[26] F. Gao, W.J. Weber, M. Posselt, V. Belko, Phys. Rev. B 69 (2004) 245205.

[27] M. Bockstedte, A. Mattausch, O. Pankratov, Phys. Rev. B 69 (2004) 235202.

[28] F. Gao, G. Henkelman, W.J. Weber, L.R. Corrales, H. Jonsson, Nucl. Instrum. Methods Phys. Res. B202 (2003) 1-7.

[29] R.J. Price, J. Nucl. Mater. 48 (1973) 47-57.

[30] S. Kondo, Y. Katoh, L.L. Snead, J. Nucl. Mater. 382 (2008) 160-169.